CHARACTERIZATION OF SURFACE DISCHARGE SWITCHES AND HIGH PERFORMANCE APPLICATIONS*

R. E. Reinovsky, J. H. Goforth, and A. E. Greene
Los Alamos National Laboratory
Los Alamos, NM 87545

J. Graham
Maxwell Laboratories, Inc.
San Diego, CA

Abstract

Results of experiments which were conducted to characterize the performance of a surface discharge as a high-performance, self-closing isolation switch for high energy applications are described. These experiments, conducted under both DC and pulsed conditions, lead to a model of switch operation which enables the design of such switches for multi-megajoule operation. The paper describes the successful implementation of a surface switch as an operational component in a multi-megampere pulse-power system.

The Surface Discharge Switch

The physical arrangement of a surface discharge switch is shown in Fig 1.

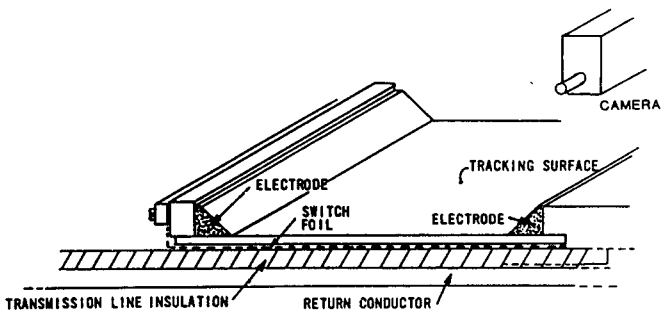

Figure 1. Physical configuration of the switch.

The essential components include a pair of electrodes, an insulator (the surface of which separates the electrodes), and a conductor located below the tracking surface which carries the circuit's return current. In general, the return conductor also establishes the electric-field distribution in the dielectric and at the air/dielectric interface. While the precise shape of the electrodes appears to be relatively unimportant, the polarity of the electrodes with respect to the return conductor and particularly the electric field at the insulator/air interface are significant. In order to provide some control over the electric-field distribution in and near the insulator surface, a thin-foil conductor is incorporated in a practical switch. The foil is connected to one electrode and extends under some thickness of the insulations and under, but insulated from, the opposite electrode. The depth at which this foil was positioned in the insulation assembly provides control of the field distribution.

DC Stress

The electrical characteristics of surface-tracking gaps were explored as a function of gap length and of the thickness and composition of the dielectric when DC stress was applied to the gap. "Breakdown" was identified with the voltage at which the gap closed as the DC voltage was ramped upward at the (relatively slow) rate of 2-5 kV/s. The breakdown voltage was measured as a function of electrode separation over the range of 0.02 to 1 meter. A variety of dielectric materials including polycarbonate, polyester (Mylar) and polyethylene in several thicknesses was used in the tests and the details of these assemblies are described in Table I.

Table I. D.C. Breakdown Tests

TEST	MATERIAL	ε_R	THICK cm	C_{sp} pF/sq cm
A	Polycarbonate (3/8")	3.2	0.953	0.296
B	Polycarbonate (1/4")	3.2	0.635	0.443
C	Polyethylene (0.130")	2.2	0.330	0.568
D	Polycarbonate (1/8")	3.2	0.318	0.887
E	Mylar (0.005" x 6)	3.0	0.0762	3.46
F	Mylar (0.005" x 5)	3.0	0.0635	4.16
G	Mylar (0.005" x 3)	3.0	0.0381	6.93
H	Mylar (0.005" x 2)	3.0	0.0254	10.4
J	Polycarbonate (0.005" x 1)	3.2	0.0127	22.2
W	Polyethylene Terefluorate	3.2	0.200	1.54
X	Polyethylene Terefluorate	3.2	0.100	3.08

Andreev[1] has reported data for a similar experiment where other dielectric materials were used and where the gap lengths ranged from about 0.25 to 2 meters. The two sets of data are plotted together in Fig. 2 over a limited (0-20 cm) range of gap lengths and are seen to display quantitatively and qualitatively similar behavior.

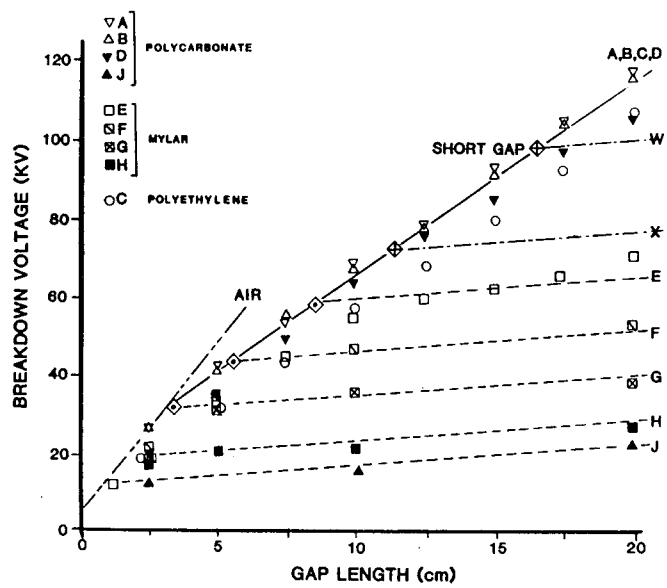

Figure 2. DC breakdown of surface switch.

Pulsed Performance

The performance of a surface switching gap was further investigated by exploring the behavior of similar electrode/insulator geometries for fast-rising,

*This work performed under the auspices of the U.S. Department of Energy.

Report Documentation Page

Form Approved
OMB No. 0704-0188

1. REPORT DATE	2. REPORT TYPE	3. DATES COVERED
JUN 1987	**N/A**	**-**

4. TITLE AND SUBTITLE	5a. CONTRACT NUMBER
Characterization Of Surface Discharge Switches And High Performance Applications Characterization	5b. GRANT NUMBER
	5c. PROGRAM ELEMENT NUMBER
6. AUTHOR(S)	5d. PROJECT NUMBER
	5e. TASK NUMBER
	5f. WORK UNIT NUMBER
7. PERFORMING ORGANIZATION NAME(S) AND ADDRESS(ES) **Los Alamos National Laboratory Los Alamos, NM 87545**	8. PERFORMING ORGANIZATION REPORT NUMBER
9. SPONSORING/MONITORING AGENCY NAME(S) AND ADDRESS(ES)	10. SPONSOR/MONITOR'S ACRONYM(S)
	11. SPONSOR/MONITOR'S REPORT NUMBER(S)

12. DISTRIBUTION/AVAILABILITY STATEMENT
Approved for public release, distribution unlimited

13. SUPPLEMENTARY NOTES
See also ADM002371. 2013 IEEE Pulsed Power Conference, Digest of Technical Papers 1976-2013, and Abstracts of the 2013 IEEE International Conference on Plasma Science. Held in San Francisco, CA on 16-21 June 2013. U.S. Government or Federal Purpose Rights License

14. ABSTRACT
Results of experiments which were conducted to characterize the performance of a surface discharge as a high-performance, self-closing isolation switch for high energy applications are described. These experiments, conducted under both DC and pulsed conditions, lead to a model of switch operation which enables the design of such switches for multi-megajoule operation. The paper describes the successful implementation of a surface switch as an operational component in a multimegampere .

15. SUBJECT TERMS

16. SECURITY CLASSIFICATION OF:			17. LIMITATION OF ABSTRACT	18. NUMBER OF PAGES	19a. NAME OF RESPONSIBLE PERSON
a. REPORT	b. ABSTRACT	c. THIS PAGE			
unclassified	**unclassified**	**unclassified**	**SAR**	**4**	

pulsed electric stress. A fast-rising voltage pulse was delivered to a gap similar to that in Fig. 1 from a small Marx generator via a peaking circuit (CLC oscillator) as shown in Fig. 3. The value of the capacitor C_2 was chosen to be much greater than the capacitance of the gap hardware so that the voltage waveform was largely independent of the details of the switch gap, especially of the gap length and the C_{sp} of the insulation. The time constant of the CLC circuit was varied by changing the value of the inductor, L, in order to evaluate the performance of the gap under voltage stresses with different time histories. Using the test circuit, it was possible to obtain "1-cosine" voltage waveforms with a rate of voltage rise of 1.39 kV/ns, 0.735 kV/ns and 0.417 kV/ns averaged along the steep part of the waveform.

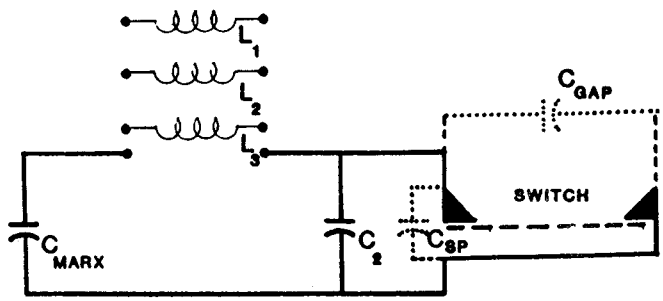

Figure 3. CLC test circuit.

Voltage histories for a 15-cm-long gap insulated with 20 sheets of 0.005" mylar (1.04 pF/cm^2) are shown in Fig. 4 for tests with three different risetimes. From the DC data in Fig. 2, we might expect such a gap to close at about 90 kV. In Fig. 4 we identify "breakdown" with the rapid collapse of gap voltage. The figure shows that the peak voltage, just before breakdown, ranges from 130 to 200 kV and that the peak voltages decrease monotonically with increasing risetime. Thus the data tentatively suggest a strong dependence of the breakdown process on the voltage stress time.

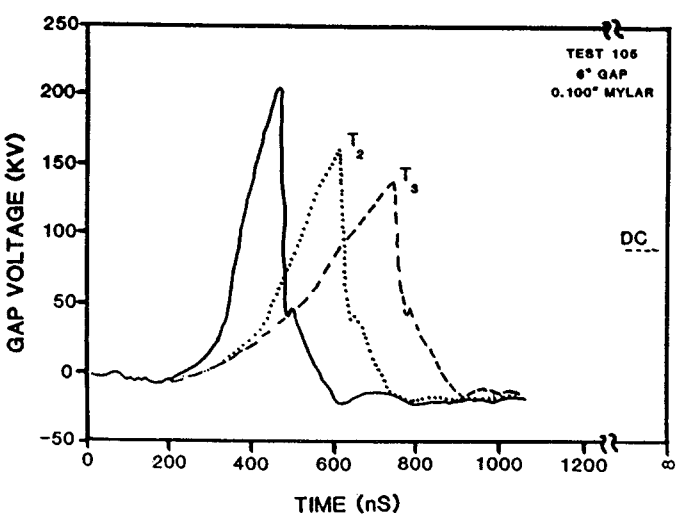

Figure 4. Voltage waveforms for three risetimes.

When the same voltage-time histories are replotted in Fig. 5a with the time reference taken as the point of collapse of gap voltage, the data show the interesting result that all three voltage-time histories intersect at a point 91 ns prior to breakdown, regardless of voltage risetime. Furthermore, the voltage at which the three waveforms cross is about 105 kV which differs from the voltage at which the DC gap breaks by only 15%.

The data in Fig. 5 is consistant with a "streamer growth" model for breakdown under pulsed stress. Figure 5 may be interpreted by observing that, for a fixed gap length, gap closure occurs at fixed time after the rising voltage has crossed some value which is independent of pulse shape. This is precisely the behavior to be expected for a streamer mechanism in which the process does not begin until the stress in the gap exceeds a threshold voltage. Subsequent to this "turn on", the streamer propagates at a velocity which is substantially independent of the magnitude of the longitudinal electric fields or of their behavior in time. The streamer mechanism is further supported by the streak photograph in Fig. 5b where the advance of the light (streamer channel) is seen to start at the time identified as the initiation time, and to reach the opposite electrode at the breakdown time following a nearly straight trajectory characteristic of a constant speed of advance across the gap. A velocity of propagation of the constant speed track can be deduced from the data in the figure and is found to be 1.67 mm/ns (15 cm/91 ns).

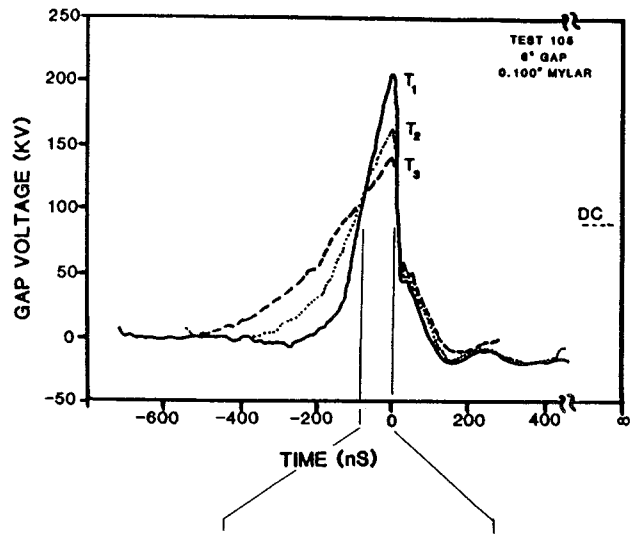

Figure 5. Voltage waveforms with common time reference at breakdown.

In Fig. 6 we plot three voltage profiles for the intermediate speed (0.735 kV/ns) circuit applied to gaps of three different lengths. In the figure we show a measurement of the time from the nominal initiation of tracking at a voltage of 105 kV to the closure of the gap, and calculate a tracking velocity of 1.66 ± 0.01 mm/ns for the three gap lengths. The close agreement between tracking velocities for gap lengths which differ by more than a factor of two further reinforces the notion that, after initiation, the track proceeds at a fixed tracking velocity that is independent of the longitudinal electric field.

Data similar to those analyzed in Figs. 4, 5, and 6 were collected over the available range of voltage risetimes, for a variety of dielectric materials and thicknesses, and for several gap lengths. Plots of voltage histories similar to the example in Fig. 5 were made to arrive at values of initiation voltage and

tracking time. A summary of the results is contained in Table II.

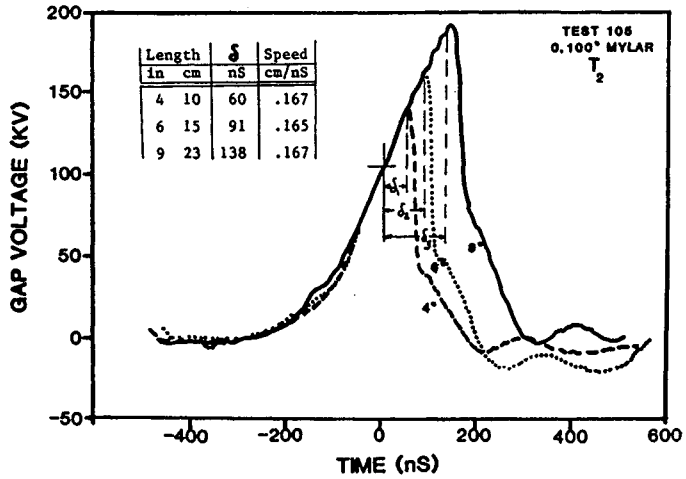

Figure 6. Voltage waveforms for three gap lengths.

Table II. Pulsed Breakdown Tests

TEST	MATERIAL	C_{sp} pF/sq cm	V_{init} kV	Vel_{track} cm/ns
POSITIVE GAP VOLTAGE				
1	Polypropylene (1/4")	0.320	180	0.242
2	Polycarbonate (1/4")	0.443	150	0.210
3	Mylar (0.005" x 20)	1.04	105	0.166
4	Common Glass (1/4")	1.05	98	0.174
5	Polycarbonate (0.005" x 5)	4.43	76	0.150
6	Polycarbonate (0.005" x 2)	11.2	42	0.072
7	Polycarbonate (0.005" x 1)	22.2	24	0.034
NEGATIVE GAP VOLTAGE				
8	Polycarbonate (1/4")	0.443	-160	0.348
9	Polycarbonate (0.005" x 5)	4.43	-72	0.193

The general behavior of the data is clearly monotonic with the parameter C_{sp} with increased specific capacitance resulting in both lower track initiation voltages, and lower tracking velocities.

Tests 8 and 9 duplicate tests 2 and 5 with the polarity of the source reversed so that the electrode which experiences high electric field in air (the electrode from which the streamer grows) is at a negative potential with respect to the return conductor. Though only two cases are presented, they suggest that reversing polarity leaves the track initiation voltage almost unaffected, but does seem to increase the tracking speed (by as much as 30%). While the negligible effect on initiation voltage is somewhat surprising, the enhancement of tracking speed is easily attributed to the fact that the (now negative) plasma at the nose of the streamer channel is an easy source of electrons which can enhance ionization just in front of the channel. Thus for the same waveform and gap geometry, the reversal of polarity would result in closure at a voltage that is on average lower (because the track moves faster and closes sooner) than that observed with positive polarity despite the fact that the initiation voltage is unchanged.

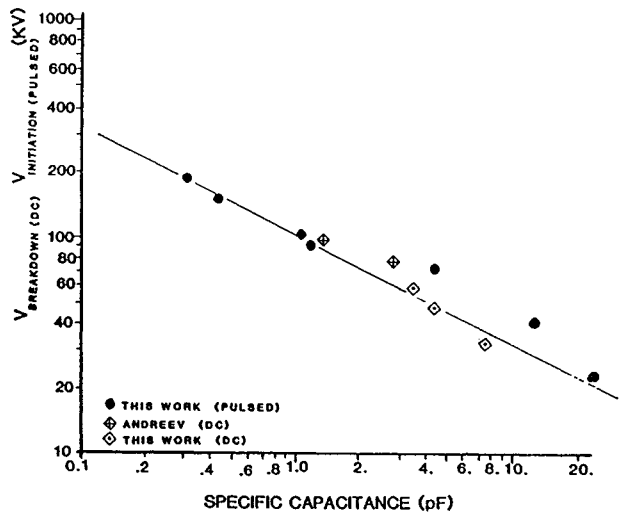

(a)

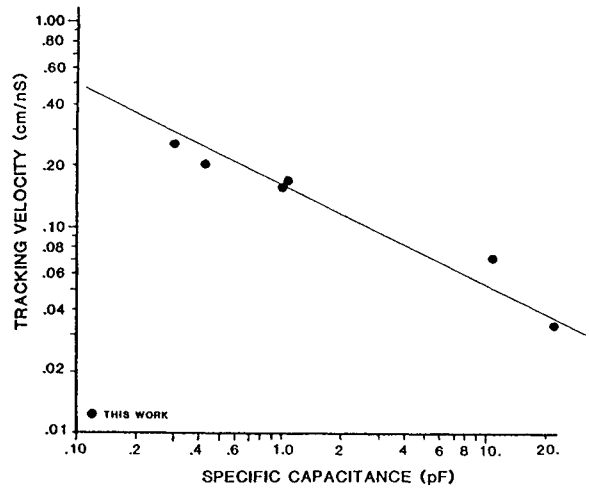

(b)

Figure 7. Track initiation voltage and tracking velocity.

In Fig. 7a we have plotted the track initiation voltages for tests 1 through 7 from Table II as a function of C_{sp}, and for comparison, we have included the "transition" points from Fig. 2. We observe that the same $C_{sp}^{-1/2}$ behavior that described the DC breakdown data continues to be useful in describing the pulsed track initiation data. In comparing the DC and pulsed data, care should be taken to note that the lines on Fig. 2 are fits to the data in the limits of long and short gaps and that the intersections of the family of short gap data with the family of long gap data (the "transition" points) represent transitions from one behavior to another and are, in fact, not good approximations to the actual DC breakdown voltages in the transition regions (which may be up to 10% lower). In Fig. 7b we plot the tracking velocity (pulsed data only) also as a function of C_{sp} and while there is some scatter in the data, the tracking velocity is seen to be at least generally described by:

$$Vel_{track} = 0.16\ C_{sp}^{-1/2}\ (cm/ns) \qquad (1)$$

Thus a relatively straight-forward approach emerges for the design of a surface switch to close at a given voltage. Armed with the empirical relation-

ships in Fig. 7, and recalling that the process is one of tracking beginning at some voltage, and proceeding with some characteristic speed relatively independent of the longitudinal field, it is possible to select a dielectric system (C_{sp}) strong enough to prevent failure prior to the desired track initiation voltage, and a gap length such that the delay from track initiation to closure provides switching action at the appropriate time in the operation of the circuit.

High Current Performance

In order to seriously evaluate a switch based on surface discharge processes for routine, high energy operation, it is necessary to consider, not only the detailed time- and voltage-dependent behavior of the discharge during the breakdown process, but also to consider the behavior of the fully developed surface discharge under conditions where the channel is carrying large currents and where the issues of switch inductance and resistance are among the important concerns.

A high current experiment was performed in cylindrical geometry using an explosive pulsed-power system consisting of a flux compression generator which delivered about 4 MA to an explosively formed fuse opening switch. A 20 nH inductive load was isolated from the fuse by a cylindrical surface tracking switch. The mechanical arrangement is shown in Fig 8.

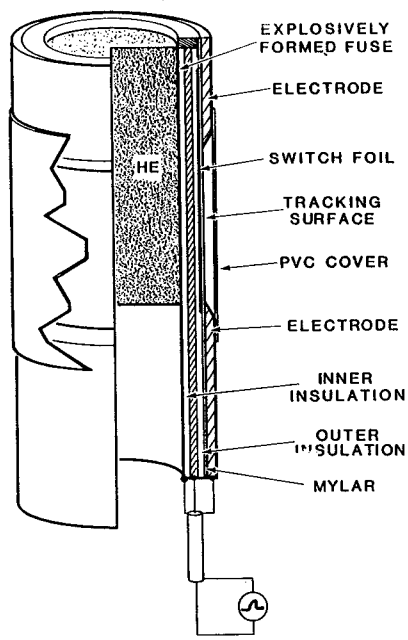

Figure 8. Physical configuration of high current experiment.

The switch was built of aluminum electrodes spaced 11 cm apart and the switch foil, connected to the negative electrode, was located below 30 mils of Mylar to form a "positive gap". The cylindrical switch had a circumference of 81 cm. In addition, a clear 0.16-cm-thick PVC sheet was wrapped around the outside of the 1.6-cm-thick electrodes to reduce the radial "lift off" of the surface switch channels. The current through the switch and the load and the voltage measured across only the switch gap are shown in Fig 9a. Dividing the switch voltage by the load current, we obtain the switch impedance shown in Fig. 9b. In the figure, the impedance is seen to reach a minimum of about 1 mΩ. In addition to electrical diagnostics, an Imacon 790 framing camera was used to view the switch during operation. The frame showed initially 10 bright channels, and by 600 ns later about 30 channels had formed. Ultimately these 30 channels carried 2.5 MA or about 80 kA/channel.

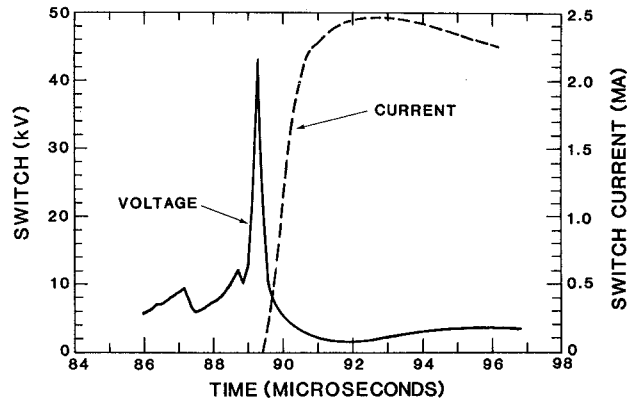

(a)

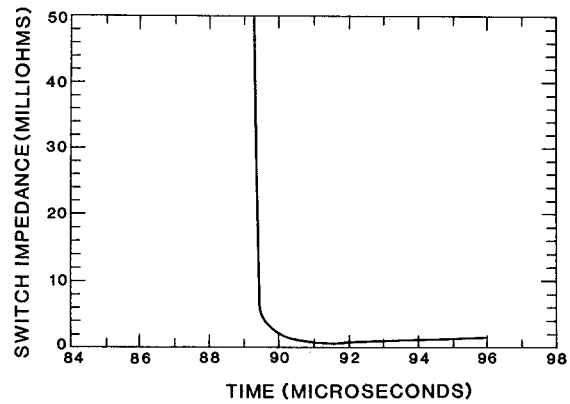

(b)

Figure 9. High current performance of surface switch.

Conclusions

Experiments which explore the breakdown behavior of self-closing surface tracking switches are reported. The breakdown mechanism was observed to follow different behavior in each of three regions, and the long gap-streamer mechanism is probably the most controllable. The long-gap mode can be characterized in terms of a track initiation voltage, and a tracking velocity, and armed with that information, switches have been designed that work at voltages of hundreds of kilovolts and megampere currents.

Acknowledgement

The support of the Air Force Weapons Laboratory, Air Force Systems Command, where some of the experiments were conducted is gratefully acknowledged.

References

[1] S. I. Andreev, E. A. Zobov, and A. N. Sidorov, "Investigation of Sliding Spark in Air, translated from: Zhurnal Prikladnoi Mechaniki i Teknicheskoi Fiziki, 3, pp. 38-43.

[2] S. I. Andreev, E. A. Zobov, A. N. Sidorov, and V. D. Kostovsov, "An Investigation of a Long Sliding Spark", translated from: Zhurnal Prikladnoi Mechaniki i Teknicheskoi Fiziki, 1, pp. 111-115.